We are IntechOpen, the world's leading publisher of Open Access books Built by scientists, for scientists

4,800
Open access books available

122,000
International authors and editors

135M
Downloads

Our authors are among the

154
Countries delivered to

TOP 1%
most cited scientists

12.2%
Contributors from top 500 universities

CLARIVATE ANALYTICS BOOK CITATION INDEX INDEXED

WEB OF SCIENCE™

Selection of our books indexed in the Book Citation Index in Web of Science™ Core Collection (BKCI)

Interested in publishing with us?
Contact book.department@intechopen.com

Numbers displayed above are based on latest data collected.
For more information visit www.intechopen.com

14

Finite-Size Effects in Graphene Nanostructures

Antonio Monari[1,2] and Stefano Evangelisti[1]
[1]*Laboratoire de Chimie et Physique Quantiques. Université de Toulouse et CNRS.*
[2] *Equipe de Chimie et Biochimie Théoriques, SRSMC, CNRS, Nancy-Université*
France

1. Introduction

Since its characterization in 2004 [Novoselov et al. (2004; 2005)] graphene has emerged as a material showing somehow rather unusual and particular characteristics [Castro Neto et al (2009); Geim (2009); Katselnson et al. (2006)]. In October 2010 A. Geim and K. Novoselov have been awarded the Physics Nobel Prize for the characterization of graphene. Much of this particular behavior is due to its nature of a pure two dimensional (2-D) materials made up of Carbon atoms in a honeycomb lattice. Moreover graphene, can be thought not only as the constituting material of the well known graphite (made up of a series of graphene stacks kept together by weak van der Waals bonds), but also as the constituent of other carbon-based nanomaterial. For instance the well known carbon nanotubes [Charlier et al. (2007)] can be considered as a rolled-up graphene sheet where edges have been joined. Fullerene [Andreoni (2000)] on the other hand can be seen as graphene with the presence of pentagonal defects responsible for the positive curvature that leads to the spherical geometry. Despite its importance, and despite the fact that graphene sheets could be produced every time someone uses a graphite-pencil, graphene was isolated and characterized only very recently, due to the technically difficulties in evidencing its formation. Moreover, even if theoretical considerations on the electronic structures of a single graphite sheets date back to the work of Pauling in 1950s [Pauling (1972)], the existence of a purely 2-D systems was considered as impossible until recently. However, soon afterwards its characterization graphene has open the way to an impressive mole of experimental and theoretical studies (see for instance Castro Neto et al (2009) and reference therein), in particular because of its remarkable electronic properties that make graphene a very important material to be exploited in the field of molecular and nano-electronics. Technical applications of graphene, or graphene-based devices, can go from single molecule detection [Schedin et al. (2007)], to field effect transistors [Novoselov et al. (2004)] and quantum information processing [Trauzettel et al. (2007)]. One should also cite that the robustness of the σ skeleton of graphene makes it one of the strongest materials ever tested [Lee et al. (2008)], and this fact obviously suggest the possible use of carbon-fiber reinforcements in novel composite materials. Although our work will not focus mainly on the properties of infinite graphene sheets, let us cite that graphene also proved to be a zero gap semi-metal, characterized by a very high electron mobility. Moreover, graphene is able to show unusual linearly dispersing electronic excitations: the electronic excitations in the vicinity of the Fermi level remind those of massless Dirac fermions. Graphene, therefore, allowed predictions of quantum electrodynamics to be tested in a solid-state system. It is also noteworthy to cite that many of these findings have been

anticipated in the framework of independent electrons band theory by Wallace back in 1947 [Wallace (1947)]. Since then, even if theoretical works have become much more accurate and have benefit of the possibility to compare to experiments, the role of electron-electron correlation in graphene has been still an object of intense debate [Castro Neto et al (2009)]. Another very interesting problems, strongly related to electronic properties and to the Dirac fermions, concerns the influence and effects produced by disorder in the physics of electrons in graphene as well as its transport properties. Some of the parameters developed in the following of this Chapter, and in particular the localization tensor, could be of seminal importance in elucidating these effects.

If, as we have briefly recalled, infinite graphene presents absolutely remarkable properties, also finite-size systems (nano ribbons or nano islands) show a behavior that needs a careful investigation [Berger et al. (2006)]. In particular the geometry of the islands, and especially the form of edges, can module the properties of the system in a very impressive way [Castro Neto et al (2009)]. We would like to stress that in the near past the control over the nano-islands geometry was rather poor, due to the fact that graphene was produced by a top-down approaches by stripping away sheets from graphite. Today, on the other hand, with the emergence of bottom-up approaches, based on controlled deposition on metallic surfaces (for instance Ruthenium), the control of the final system geometry has significantly improved, and it is now possible to produce nano-islands of different size and forms with atomically defined edges [Fernandéz-Rossier & Palacios (2007)], ranging from the quasi-one dimensional ribbons to the zero-dimension dots. One of the first and better known and studied finite-size effect on graphene is the emergence of edge-states in the case of nano-ribbons [Son et al. (2004)]. From a physical points of view this means that the electrons close to the Fermi level tend to preferentially occupy regions of space that are close to the borders of the ribbon. This feature has been observed experimentally and has been predicted with high level *ab initio* computations for instance by Hod et al. (2008; 2007). It is also known that the behavior of the nano-ribbon strongly depends on the type of edges, giving rise to the two well known classes of "zig-zag" and "armchair" edges. More complex structures, such as hexagonal, rhomboidal and triangular ones, will show an even more complex behavior and can also give rise to open shell, high multiplicity ground states [Fernandéz-Rossier & Palacios (2007); Yu et al. (2008); Ezawa (2007)]. This could result in the possibility of rationally design advanced nano-magnets, also exploiting the connection of different multiplicity sub-units (see for instance the works of Yu et al. (2008); Trinquier et al. (2010)). In the same way, as suggest by Fürst et al (2009) the possibility to create antidot graphene lattices, in which graphene can be artificially periodically perforated to create a precise arrangement of holes, appears very promising to further control and module electronic properties. All this attempts can be seen as steps toward the production of metametarials [Pendry et al. (1996)], i.e. materials that derive their properties from their artificial, man-made, periodic small-scale structure. Anyway it is noteworthy to cite also all the attempts made to enhance physically properties of graphene-like structures by their interaction with atoms or small molecules, for instance following the procedure of the spin doping.

1.1 Magnetic properties of graphene nano-systems

An important feature to rationalize the relation between structure and electronic properties, and more generally, to study finite size effects on graphene nano-structures, is to recognize that the honeycomb graphene is composed by a bipartite lattice [Fernandéz-Rossier & Palacios (2007)], with two compenetrating triangular sublattices A and B. Each atom constituting the

graphene can be associated to one of the two sublattices, one can therefore speak of A and B graphene atoms or centers. Moreover, each A atom will only have B nearest neighborings and viceversa. So for instance, zig-zag edges are composed of atoms that all belong to the same sublattices, while the same does not hold for armchair edges. Moreover in order to rationalize the emergence of magnetic properties in graphene nanosystems one can recall the Lieb's theorem [Lieb (1989)]. This theorem, also known as the theorem of itinerant magnetism and usually applied within the framework of the Hubbard one-orbital model, is indeed intended to predict the total spin of the ground state in bipartite lattices. In particular one can see that an imbalance on the number of atom in one sublattice will yeld a magnetic ground state with spin

$$S = \frac{|N_A - N_B|}{2} \tag{1}$$

where N_A and N_B are the numbers of atoms of A and B type respectively. Moreover, in a Hückel type approximation, $|N_A - N_B|$ will also be the number of eigenvalues equals to zero. It is also important to note that the magnetization originating from localized edge-states give also rise to a high density of states at the Fermi level which in turn can determine a spin polarization instability. Moreover the relation between the unbalanced number of atoms and the ground state spin implies that two centers will be ferromagnetically coupled if they belong to the same sublattice and antiferromagnetically coupled if they do not [Yu et al. (2008)].
If now we will consider triangular type nanoislands (as will be evident in the following sections) one can see that the two sublattices are unbalanced, i.e. $N_A \neq N_B$. For this reason, the fundamental ground state will be a magnetic one, as was confirmed for instance by Fernandéz-Rossier & Palacios (2007). When, on the other hand, one deals with hexagonal coronene-like structures $N_A = N_B$, the ground state will be a closed shell singlet. In particular, in the latter case no eigenvalue of the Hückel Hamiltonian will be equal to zero. In reality, since even if a gap still exist at the Fermi level, increasing the size of the hexagonal island will diminish the difference between the highest occupied and the lowest unoccupied molecular orbitals (HOMO, LUMO), thus favoring an open-shell solution. Indeed a quantum phase transition has been predicted for hexagonal structures leading to a compensated ferrimagnet [Yu et al. (2008)].
In the following, we will rationalize the relation between magnetic and electronic properties of graphene nanostructures, presenting also a comparison between the simple Hückel, tight-binding, Hamiltonian and more sophisticated multireference *ab initio* ones.

1.2 Modern theory of conductivity: Polarizability and localizability

Graphene and graphene nano-ribbons are known to exhibit a very particular and in some cases exotic electronic properties [Castro Neto et al (2009)]. Graphene, for instance, is very well known for being a zero-gap semiconductor, characterized by an infinite electron mobility. Finite graphene nanoribbons, or Graphene Nano Islands (GNI), on the other hand show electronic properties that can vary drastically with the geometrical structure and shape [Castro Neto et al (2009); Fernandéz-Rossier & Palacios (2007); Yu et al. (2008)]. For these reasons, a study of electronic properties of GNI in the framework of the modern theory of conductivity [Resta (1998); Resta & Sorella (1999)] can be of valuable importance in order to elucidate the characteristic of these systems, as well as their correlation with the shape, as was recently pointed out by Evangelisti et al. (2010).
For readers' convenience, we report here a brief review of the so called modern theory of conductivity, explicitating the most relevant quantities appearing in this formalism to

discriminate between a metal and an insulator.
Modern theory of conductivity first emerged in a well established way with the seminal works of Kohn in 1964 [Kohn (1964)]. In this work, for the first time, the character of an insulating state was related not only to the few electronic states close to the Fermi level, as it was customary on the "classic" theory, but indeed to the ground state as a whole. To use Kohn's words, *"insulator behavior does not appear to depend on the notion of a filled band, but rather reflects a certain type of organization of the electrons"*. Going even further, Kohn affirms that in the insulating state the electrons *"so organize themselves as to satisfy a many electron localization condition"*.
Therefore, one can understand that, in this framework, the emergence of a metallic or insulator behavior is no more related to the opening or closing of a gap at Fermi level but indeed to the emergence of electron localization or delocalization [Resta & Sorella (1999); Kohn (1964)].
Different authors contributed to the development of the theory in the last years, and in particular the localization condition invoked by Kohn was given a quantitative indicator by means of the localization tensor, as defined by Resta and Sorella [Resta (1998); Resta & Sorella (1999); Aoki & Imamura (1995)]. Although this theory was first derived within Periodic Boundary Condition, its extension to the case of finite systems is possible, and is clearly much more appropriate for the systems we want to investigate here [Resta (2005; 2006)].
Suppose we consider an electronic wavefunction $|\Psi>$, and indicate by $\hat{\mathbf{r}}_i$ the position operator of the i-th electron (the position operator being a vector quantity of Cartesian components x, y, z). Then $\hat{r_\beta}$ will be one Cartesian component of the total position operator

$$\hat{\mathbf{r}} = \sum_{i=1}^{n} \mathbf{r}_i \tag{2}$$

It will be possible to define the localization tensor (or localizability) of the state associated to $|\Psi>$ as the cumulant of the second-order momentum with respect of the operator $\hat{\mathbf{r}}$ i.e. the quadratic fluctuation of the position

$$< r_\beta r_\gamma >_c = \frac{1}{n} (< \Psi|\hat{r}_\beta \hat{r}_\gamma|\Psi > - < \Psi|\hat{r}_\beta|\Psi >< \Psi|\hat{r}_\gamma|\Psi >) \tag{3}$$

Notice that the $\frac{1}{n}$ factor has been introduced in order to eliminate the dependence on the number of electrons n in the case of identical *non interacting* subsystems. In the following, for the sake of simplicity of notation, the locality-tensor components $< r_\beta r_\gamma >_c$ will be simply indicated as $\rho_{\beta\gamma}$ and the definition of Localizability will be used in analogy with polarizability. As shown by Resta [Resta & Sorella (1999)]in the case of a metallic system the locality ρ will diverge, while for insulators it will converge to a finite value. We will also remind that the locality has been directly related to the macroscopic conductivity $\sigma(\omega)$ by Souza et al. (2000)

$$\rho_{\alpha\beta} = \delta_{\alpha\beta} \frac{V}{n} \frac{\hbar}{\pi e^2} \int_0^\infty \frac{d\omega}{\omega} \Re\sigma(\omega) \tag{4}$$

An equivalent, in the case of a complete expansion space, and in some instances more convenient expression of the localization tensor can be obtained by invoking the sum-over-states or spectral resolution formalism as:

$$\rho_{\alpha\beta} = < \Psi_0|(r_\beta - < r_\beta >)|(r_\gamma - < r_\gamma >)|\Psi_0 > = \sum_{k>0} < \Psi_0|r_\beta|\Psi_k >< \Psi_k|r_\gamma|\Psi_0 > \tag{5}$$

Here the vectors $|\Psi_k>$ are the (excited) eigenvectors of the system while $|\Psi_0>$ represents the ground state. In this formalism the relation between polarizability and locality becomes much more evident if one recall the spectral resolution form of the (static) polarizability:

$$\alpha_{\beta\gamma} = 2\sum_{k>0}\left(\frac{<\Psi_0|r_\beta|\Psi_k><\Psi_k|r_\gamma|\Psi_0>}{E_k - E_0}\right) \tag{6}$$

where E_k are the eigenvalues corresponding to the Ψ_k eigenvector, E_0 being the ground state energy. We will also recall that for conducting systems too the polarizability will diverge, implying, from a more physical point of view, and infinite possibility of deformation of the electronic cloud of the systems.
Hence, the metallic or insulator characteristic of a system can be investigated by three criteria:

1. Zero energy gap.
2. Infinite per-atom polarizability.
3. Infinite fluctuation of the position operator (Localizability).

Anyway, it has to be pointed out that while the energy gap relates the metallic behavior of a system only to the states close to the Fermi level the polarizability and the Localizability are able to-take into account the properties of the whole system as it is clear from the spectral-resolution formalism.
We would also like to remind that, strictly speaking, since we are dealing with finite systems, it is clearly impossible to obtain a true metallic behavior. However, the divergent or convergent behavior of the Localizability (and of the per-atom - or Specific - Polarizability) can be clearly evidenced. Therefore, one can reasonably speak of a sort of metalicity, or at least of the presence of "precursors" of metallic characters.

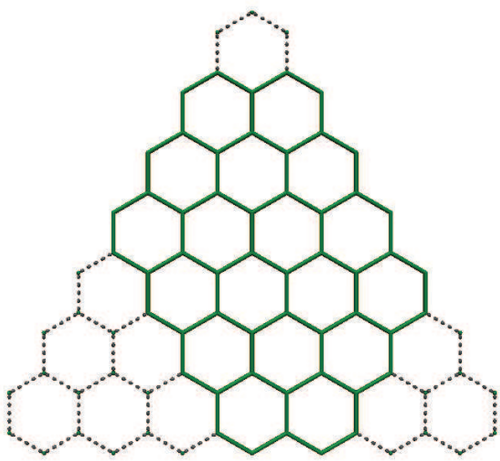

Fig. 1. The $(7|3,2,1)$ HGNI. Note that the triangles eliminated from the original hypertriangulene structure have been represented with dots

The previous formalism has already been applied to the study of metal insulator transition in different systems, both at *ab initio* [Vetere et al. (2008)] and tight binding level [Evangelisti et al. (2010); Monari et al. (2008); Bendazzoli et al. (2010)] and it has been shown that the equivalence of the previous cited criteria does not always hold. For instance, disordered [Bendazzoli et al.

(2010)] systems are gapless while being insulator, and graphene nano-ribbons [Evangelisti et al. (2010)] can show a divergent polarizability and a convergent localizability. For this reason, modern theory of conductivity proves its uselfullness in giving the possibility of a deeper characterization of the metallic and insulator states.

2. Hexagonal Graphene Nanoislands

In this section, a possible classification of GNI is proposed and illustrated. We will limit ourselves to Hexagonal GNI (or HGNI), which are defined as the convex structures that have a (*a priori* irregular) hexagonal shape. Because of the hexagonal structure of the building block of graphene, the hexagonal motifs representing HGNI will have angles of 60, 120 or 180 degrees. In order to establish a classification of HGNI, we will start from a hypertriangulene having a side containing Λ hexagons. The most general HGNI that can be derived from it well be obtained by deleting three triangular patterns out of the triangulene vertices (see Figure 1). Each one of these three triangles will be uniquely identified by the number of elementary hexagons of its side, λ_i, with $i = 1, 2, 3$. Notice that, in some cases, some of the λ_i can be zero. The resulting HGNI will then be indicated by $(\Lambda|\lambda_1, \lambda_2, \lambda_3)$. In order to avoid any ambiguity, we will assume

$$\lambda_1 \geq \lambda_2 \geq \lambda_3$$

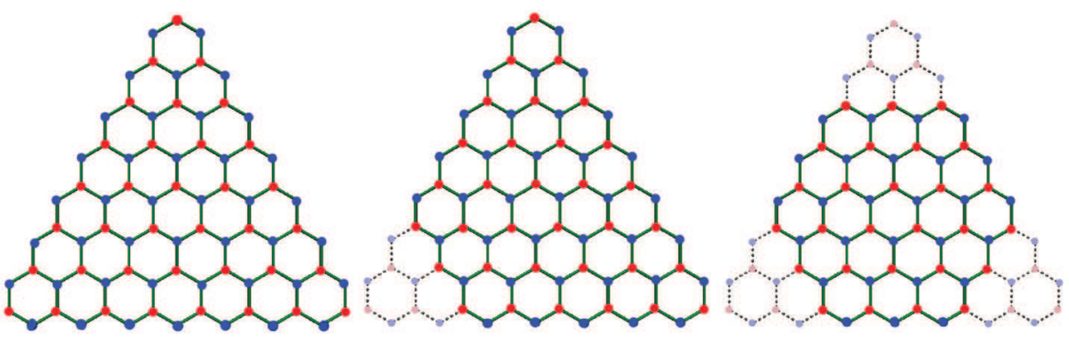

Fig. 2. The A "lateral" (dark blue) and B "apical" (dark red) sublattice sites of various HGNI. Notice in light blue and light red the eliminated lateral and apical sites, respectively, when $\lambda \neq 0$. Left the $(7|0,0,0)$ triangulene, with a lateral-apical sites difference equal to $\Lambda - 1 = 6$. Center the $(7|2,0,0)$ characterized by a lateral-apical sites difference of $\Lambda - \lambda_1 - 1 = 4$. Right the $(7|2,2,2)$ coronene that exhibits a lateral-apical sites difference of $\Lambda - \sum_i \lambda_i - 1 = 0$

Notice that, in our notation, the small triangles are not allowed to overlap. This implies that the sum of two different λ's must be smaller than (or at most equal to) Λ. Because of the ordering we have assumed, this condition is automatically fulfilled if we have

$$\lambda_1 + \lambda_2 \leq \Lambda$$

As we said in the Introduction, Graphene is a bipartite lattice. Therefore, HGNI also are obviously bipartite lattices. This implies that, at the Hückel level, the number of zero-energy orbitals is given by the difference between the two types of lattices.
Let us consider a triangulene structure. With our previous notation, it will be described as $(\Lambda|\,0,0,0)$. The lattice sites will be called "lateral" (blue in Figure 2) or "apical" (red in Figure 2). In particular, lateral sites will be defined as the Carbon atoms on one of the three edges in the $(\Lambda|\,0,0,0)$ triangulene, while the three terminal atoms will be apical.

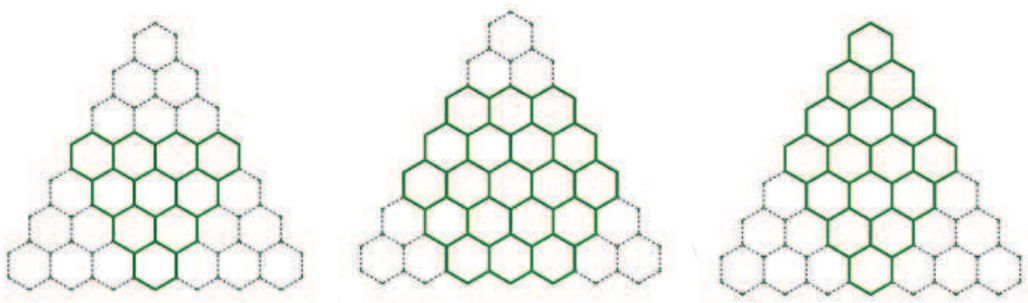

Fig. 3. HGNI obtained from the $(7|0,0,0)$ triangulene. Left the $(4|0,0,0)$ triangulene. Center the $(7|2,2,2)$ coronene. Right the $(7|2,2,0)$ pyrene. Eliminated triangles represented with dots

If one looks at Figure 2, it is straightforward to note that the difference between A and B sites is equal to the difference between lateral and apical sites. On the other hand it is also evident that the lateral sites outnumber the apical ones by $\Lambda - 1$.
When a triangular portion is cut at a triangulene vertex, the difference between the lateral and apical sites is reduced by λ. As a general result, we obtain that the difference between the lateral and apical sites (referred to the original triangulene structure) is given by

$$\Lambda - \sum_{i=1}^{3} \lambda_i - 1$$

The modulus of this quantity gives the number of zero-energy orbitals of the system if treated at the Hückel level, n_0.
It is useful to consider some special cases (see Figure 3):

- Triangulenes: They are described by the pattern $(\Lambda|\,0,0,0)$, and have $n_0 = \Lambda - 1$. They can also be obtained by cutting three identical triangular portions having side λ out an original triangulene having side equal to $2\lambda + 1$: $(2\lambda + 1|\lambda,\lambda,\lambda) = (\lambda + 1|\,0,0,0)$.
- Coronenes: They are characterized by the pattern $(3\lambda + 1|\lambda,\lambda,\lambda)$, which implies that $n_0 = 0$.
- Pyrenes: The are characterized by the pattern $(2\lambda + 1|\lambda,\lambda,0)$, which also implies that $n_0 = 0$.

Finally, we notice that HGNI having a D_{3h} symmetry are obtained if and only if the three λ_i are equal: $(\Lambda|\lambda,\lambda,\lambda)$, which gives $n_0 = |\Lambda - 3\lambda - 1|$ It is possible to start from a triangular structure and, by *adding* hexagons on the sides, to pass through a series of D_{3h} shapes, finally ending up with a larger triangulene:

$(2\lambda + 1|\lambda,\lambda,\lambda)$
$(2\lambda + 1|\lambda - 1,\lambda - 1,\lambda - 1)$
$(2\lambda + 1|\lambda - 2,\lambda - 2,\lambda - 2)$
...
$(2\lambda + 1|0,0,0)$

If λ is an integer multiple of 3, the series will pass from the coronene $(2\lambda + 1|\frac{2}{3}\lambda, \frac{2}{3}\lambda, \frac{2}{3}\lambda)$.

3. Computational details

In this Section, we will recall the computational details and strategies used in the present work. In particular the details concerning both the *ab initio* and the *tight binding* approach will be discussed.

3.1 Tight binding

All the computation at the tight binding (Hückel in the language of Chemists) level have been performed by using a specific home-made code [Evangelisti et al. (2010)]. In particular, the diagonalization of the Hückel Hamiltonian, in order to get the eigenvectors and eigenvalues, have been performed by using high efficiency BLAS and Lapack [lapack (1999)] subroutines. The Hückel Hamiltonian has been constructed starting from the connectivity of each carbon atoms in each HGNI, defining

$$\langle i|\hat{H}|i\rangle = \alpha = 0 \tag{7}$$

and

$$\langle i|\hat{H}|j\rangle = \beta\gamma_{ij} \tag{8}$$

where γ_{ij} is 1 if i and j are different sites connected in the HGNI skeleton, and 0 otherwise. We remind that $-\beta$ is sometimes called the hopping integral t in physical literature. In HGNI, due to a more complex connectivity, the Hückel Hamiltonian matrix will not be a tridiagonal one, as it is customary in model linear systems (polyacetilene).
As will be discussed in the next section for some systems by diagonalization of the Hamiltonian we obtained some strictly zero eigenvalues, in that case we considered the system as an open shell one, and each zero eigenvector was considered as a half filled orbital. Polarizability and Localizability have been computed by direct application of equations 4 and 5, anyway we would like to stress that since we are dealing also with open shell systems it was necessary to compute separately the contribution coming from spin up and spin down (α and β) electrons.

3.2 Ab initio

All the *ab initio* calculations have been performed by using the MOLPRO [Knowles & Werner (2002)] Quantum-Chemistry package. The nanostructures investigated at *ab initio* level have at least a D_{3h} symmetry. Coronene islands are more symmetric, having a D_{6h} point-group symmetry. However, most *ab initio* codes (and MOLPRO is one of these) are able to treat only abelian subgroups. Because of this symmetry constraint, calculations have been performed in C_{2v} and D_{2h} instead of D_{3h} and D_{6h}, respectively. All HGNI edges have been saturated with Hydrogens atoms.
In *ab initio* calculations, all the angles concerning connected atoms have been fixed to the ideal value of 120 degrees. The internuclear C-C distance between connected atoms was fixed at 1.4 Å, while the corresponding C-H distance was fixed at 1.0 Å.
The atomic basis set is the minimal STO-3G [Hehre et al. (1969)] contracted gaussian basis for both Carbon and Hydrogen. Although this basis set is certainly too small to give quantitatively reliable results, it is known to reproduce correctly the qualitative behavior of many organic and inorganic systems. Its reduced size, on the other hand, permits to investigate at a correlated *ab initio* level systems whose size is relatively large.

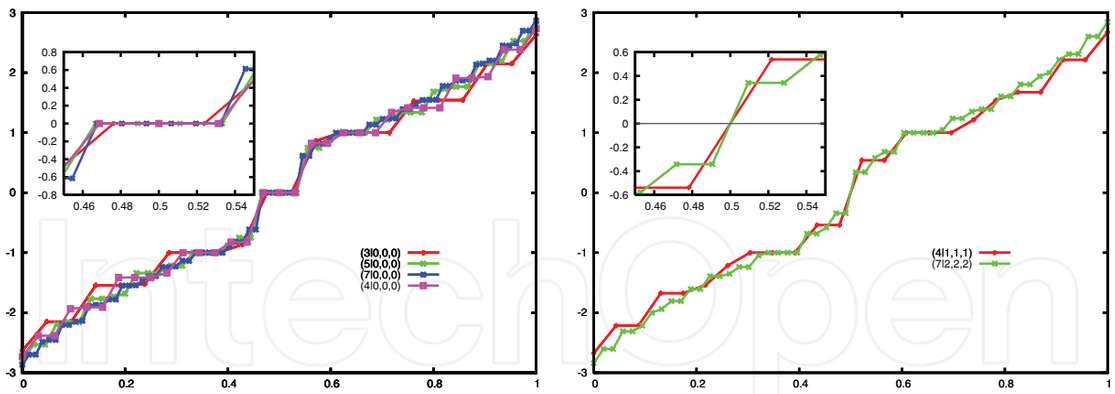

Fig. 4. The tight binding energy spectrum of some triangulene (left panel) and coronene (right panel) structures. In the boxes see a zoom of the Fermi level

The systems have been studied at Complete Active Space Self Consistent Field (CAS-SCF) level [Roos et al. (1980)], and Multi-Reference Perturbation-Theory level by using the n-electrons valence perturbation theory (NEVPT2) formalism [Angeli et al. (2001; 2002; 2007)]. In all the CAS-SCF calculations, the active space has been selected by choosing the orbitals that are strictly degenerated at Hückel level. The orbitals have been optimized at RHF level for the high-spin wavefunction. These same orbitals have been then frozen for the CAS-SCF calculations on the other spin multiplicities. In this way, our calculations are actually of CAS-CI type. The NEVPT2 formalism has then be applied to these CAS-CI wavefunctions in order to recover the dynamic correlation.

4. Results and discussion

The different behavior of Coronenes and triangulene finite size graphene structure will be illustrated in this Section. In particular we will first consider the tight binding approximation, before switching to an *ab initio* approach that allows us to better analyze the magnetic behavior of such systems.

4.1 Tight binding

Even if the tight-binding approach represents a crude approximation of a chemical systems, it can be important to sketch out some general tendencies, and to elucidate the behavior of different classes of compounds. This is particularly true since it allows the treatment of very large systems due to its extremely reduced computational cost.

The tight binding (Hückel) calculations of the different HGNI show, first of all, a quite different behavior between the triangulene and coronene classes. This difference is another confirmation of the very important role played by the finite size effects in graphene nano-islands. The energy spectra of some Triangulenes are shown in the left panel of Figure 4, while Coronenes are shown in the right panel (Notice that the spectra have been normalized with respect to the number of carbon atoms, and therefore with respect to the number of eigenvalues for graphical reasons). If the tail of the spectra looks similar between the two classes of compounds and between islands of different size, a remarkable difference can be seen at the Fermi level. As expected, [Fernandéz-Rossier & Palacios (2007); Yu et al. (2008)] Coronenes show a gap at the Fermi level, while Triangulenes shows the presence of some degenerate energy eigenvalues at the Fermi level. As can be seen on Table 1, where

system	n_C	N_f	α_x	ρ_x
(4|1,1,1)	24	0	0.37321	0.48330
(7|2,2,2)	54	0	0.62249	0.59056
(3|0,0,0)	22	2	0.40466	0.48802
(5|0,0,0)	46	4	0.53029	0.55306
(7|0,0,0)	78	6	0.64423	0.59801
(4|0,0,0)	33	3	0.46865	0.52370
(7|1,1,1)	69	3	0.71761	0.61768

Table 1. Localizability (ρ) and Specific Polarizability (α), in arbitrary units, for the tight-binding approximation; n_C indicates the number of Carbon atoms; n_0 represents the number of states at the Fermi level, i.e. having an eigenvalue exactly zero.

the number of zero level is reported, the Lieb theorem is exactly respected, as well as our empirical formula. Moreover the Lieb theorem appears also to be respected for intermediate structures like the (7|1,1,1) island, which present three zero-energy levels again as predicted from our formula. The magnetic levels arise from orbitals concentrated at the edge of the structure (edge states). This will induce a concentration of the spin density at the border of the island, as can be seen in Figure 5, where the Hückel spin density for the (7|0,0,0) triangulene has been shown. The spin density has been obtained by using Hückel eigenvectors and considering an occupation equal to one of the degenerate zero-energy eigenvalues. For graphical reasons, an arbitrary totally symmetric gaussian function has been placed on each Carbon center.

Finally if one enlarges the island the effect imposed by the different edges, and by the unbalancement of apical and lateral sites becomes less important. The HGNI energy spectrum is expected to converge toward the infinite graphene structure. In Figure 6 we report the spectra of the (121|40,40,40) coronene and of the (95|0,0,0) triangulene (both structures having about 10,000 carbon atoms). The two spectra are nearly superposable, even if a slight difference still remains in the close vicinity of the Fermi level. Indeed even if coronene will present a gap, while triangulene will be gapless, the energy difference between occupied and unoccupied orbitals in the first system will become smaller and smaller with the system size, tending to the gapless spectrum of infinite graphene. This fact can be considered as the origin of the spin instability of large coronene systems, for which the ground state will be an open shell one instead of a closed shell. In Table 1 we also report the values of the specific (i.e. per atom) polarizability and Localizability of the different classes of compounds. We can see that for small size HGNI the two parameters behave in a similar way with the

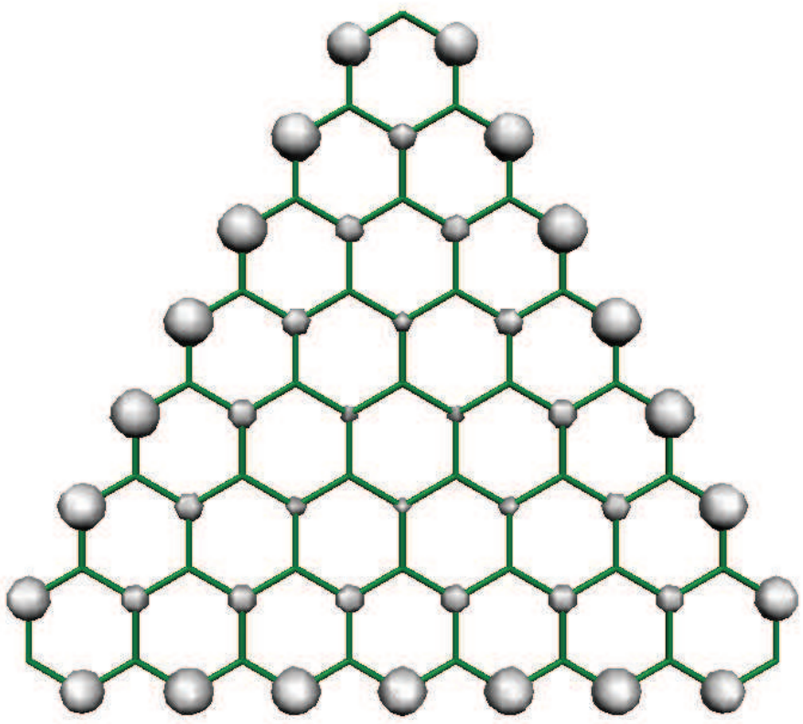

Fig. 5. The tight binding spin density of the (7|0,0,0) triangulene (septuplet state)

system size, and within the different classes of compounds although polarizability appears to have a slightly higher value than Localizability. In Figure 7 we report the behavior of specific polarizability and Localizability for triangulenes of different sizes up to the (100|0,0,0) HGNI. If Localizability appears to converge to a value close to 1, specific polarizability diverges linearly (implying an overall quadratic divergence of the polarizability). These results, which shows a qualitatively different behavior of the two indicators, can be considered to be in coherence with the observation that extended graphene is a semiconductor with infinite electronic mobility.

4.2 Ab initio

In Table 2, we report CAS-SCF and NEVPT2 computations on different graphene nano-island. In particular, as stated in Computational Details, we included in the active space the orbitals that give rise to the degenerate zero-energy manifold at tight-binding level. This choice assures to obtain a Multi-Configurational wavefunction that is able to correctly represent the physics of the problem, without presenting an explosive size of the configuration space. As it was already evident at Hückel level, the splitting of the different levels follows quite remarkably the Lieb theorem for a Hubbard bipartite lattice. Indeed, in the case of Triangulenes, the electronic state with multiplicity coherent with the Lieb theorem ($n_0 + 1$, where n_0 is the difference between apical and lateral sites) is the ground state. The same is true for the (7|1,1,1) intermediate system. In a similar way, Coronenes, at least for the size of the ones investigated here, show always a singlet ground state.

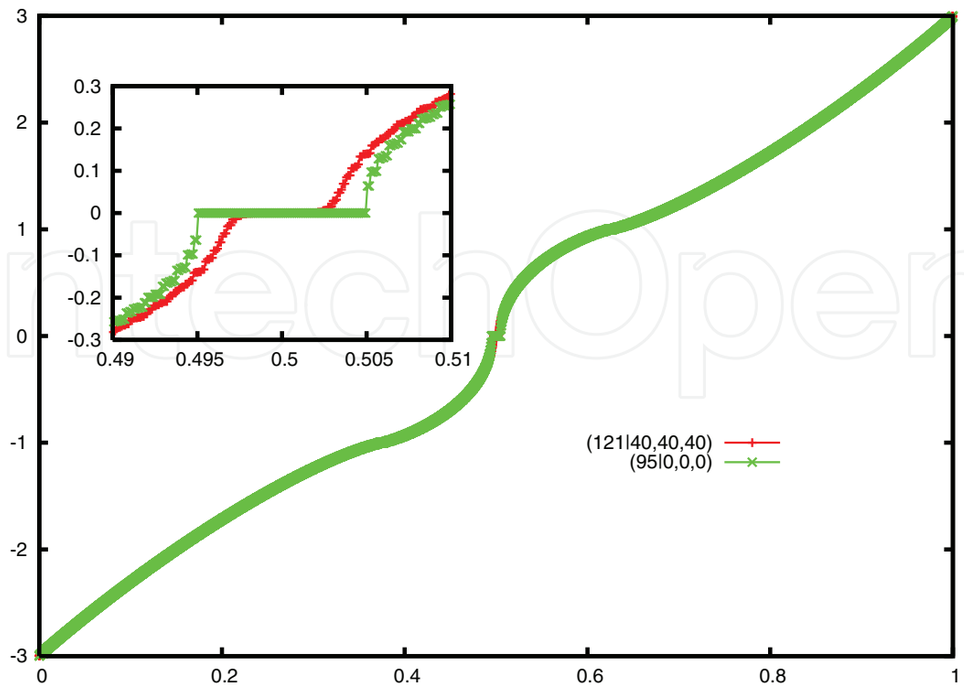

Fig. 6. The tight binding energy spectrum of (121|40,40,40) coronene and (95|0,0,0) triangulene both tending to the infinite graphene spectrum

The same effects can be seen on the left and right panel of the Figure 8, where we report the energy of the different multiplicity state, with respect to the highest multiplicity ground state, of different odd Triangulenes at CAS-SCF and NEVPT2 level.
As far as the effect of the size of the island is concerned, one can easily see that the energy splitting is large in larger structures. Therefore, one can assume that enlarging the structure will tend to favor the ferromagnetic coupling of the unpaired electrons. Rather interestingly, on the other hand, the inclusion of the dynamic correlation (at NEVPT2 level) determines a very strong lowering of the ferromagnetic coupling, up to a factor of one half in the case of odd Triangulenes. Probably this means that the relaxation of the other π double occupied orbitals induce a rather important stabilization of the low spin states. We would like to stress that, to such a magnitude, this phenomenon is quite uncommon in the magnetic spectrum of organic and inorganic magnetic materials, thus suggesting a peculiar role played by the graphene-like electronic structure.

5. Conclusion

We have reported a tight binding and *ab initio* study of graphene triangular and hexagonal nano structures. In particular, we proposed a general classification of these structures based on an index Λ and three indices λ_i. We showed how Coronene and Triangulene classes of HGNI can be easily identified within this classification via an opportune choice of the indices. By using the Lieb theorem and considering that graphene is actually a bipartite lattices, we showed how it is possible to guess the magnetic properties of these nano-structures from the values of Λ and λ_i. This heuristic findings have been confirmed also by high level *ab initio* computations. We also showed how the magnetic properties of Triangulenes structures are

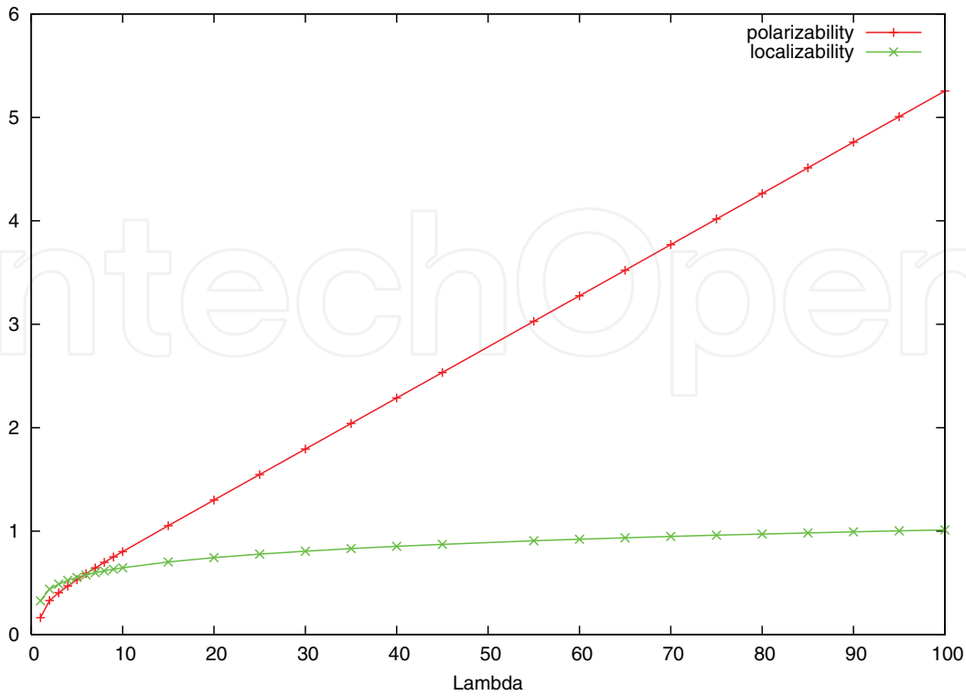

Fig. 7. The specific polarizability and Localizability of different Triangulenes $(\Lambda|0,0,0)$ as a function of Λ

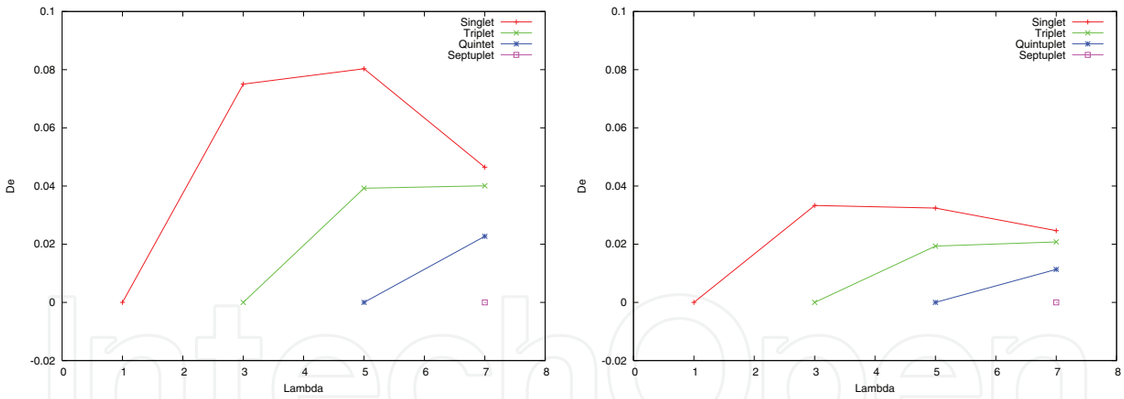

Fig. 8. The CAS-SCF (left panel) and NEVPT2 (right panel) magnetic spectrum for the odd Triangulenes with respect to the highest multiplicity ground state. Energy in hartree

given by edge states and orbitals, giving rise to a concentration of the spin density at the border. However, we underlined how the particular nature of graphene induces a specific behavior of the magnetic spectrum. In particular, the ferromagnetic coupling is very strongly reduced by the inclusion of dynamical correlation.

The behavior of graphene nano-islands has also been studied in the framework of the modern theory of conductivity, in particular by using the localization tensor (Localizability) and the polarizability. We showed how, in the limit of an extended graphene sheet, the two indicators of a metal-insulator transition behave in a qualitatively different way: while polarizability diverges Localizability shows a convergence. This fact can be ascribed to the nature of

system	n_C	n_H	S	E_{CAS-CI}	E_{NEVPT2}
(4|1,1,1)	24	12	1	0.00000000	0.00000000
(7|2,2,2)	54	18	1	0.00000000	0.00000000
(3|0,0,0)	22	12	3	0.00000000	0.00000000
			1	0.07504935	0.03331113
(5|0,0,0)	46	18	5	0.00000000	0.00000000
			3	0.03924909	0.01935507
			1	0.08033144	0.03242700
(7|0,0,0)	78	24	7	0.00000000	0.00000000
			5	0.02271725	0.01135881
			3	0.04009214	0.02078559
			1	0.04647274	0.02467302
(4|0,0,0)	33	15	4	0.00000000	0.00000000
			2	0.03632651	0.02469043
(7|1,1,1)	69	21	4	0.00000000	0.00000000
			2	0.00466476	0.00624823

Table 2. Relative Energies (hartree) of nanoislands species, computed at *ab initio* level:

extended graphene, that is known to behave like a gapless semi conductor with infinite electron mobility. These results also confirm how the use of modern theory of conductivity can be of valuable importance in the study of exotic materials.

6. Acknowledgments

The authors would like to kindly acknoweldge support from the University of Toulouse and Nancy and from the French CNRS, also under the PICS action 4263. Support from European Union under the Cost in Chemistry Actions D37 (GRIDCHEM) and CM0702 is also gratefully acknoweldged.

7. References

K. S. Novoselov, A. k. Geim, S. V. Morozov, D. Jang, Y. Zhang, S. V. Dubonos, I. V. Grigorieva, A. A. Firsov"Electric Field Effect in Atomically Thin Carbon Films" Science 306 666 (2004).

K. S. Novoselov, A. K. Geim, S. V. Morozov, D. Jang, M. I. Katselnov, I. V. Grigorieva, S. V. Dubonov, A. A. Firsov "Two-dimensional gas of massless Dirac fermions in graphene" Nature 438 197 (2005).

A. H. Castro Neto, F. Guinea, N. M. R. Peres, K. S. Novoselov, A. K. Geim, "The electronic property of graphene" Rev. Mod. Phys. 81 109 (2009).
A. K. Geim "Graphene: Status and Prospects" Science 324 1530 (2009).
M. I. Katselnson, K. S. Novoselov, A. K. Geim "Chiral tunnelling and the Klein paradox in graphene" Nat. Phys. 2 620 (2006).
J. C. Charlier, X. Blase, S. Roche "Electronic and transport properties of nanotubes" Rev. Mod. Phys. 79, 677 (2007)
W. Andreoni "The physics of Fullerene-Based and Fullerene Related Materials" Springer Berlin (2000).
L. Pauling "The nature of chemical bond" Cornell University Press, Ithaca, NY (1972).
F. Schedin, A. K. Geim, S. V. Morozov E. W. Hill, P. Blake, M. I. Katselson, K. S. Novoselov "Detection of individual gas molecules adsorbed on graphene" Nat. Mater. 6 652 (2007)
B. Trauzettel, D. V. Bulaev, D. Loss, G. Burkard "Spin qubits in graphene quantum dots" Nat. Phys. 3 192 (2007).
C. Lee, X. Wei, J. W. Kysar, J. Hone "Measurement of the Elastic Properties and Intrinsic Strength of Monolayer Graphene" Science 321 385 (2008).
P. R. Wallace "The Band Theory of Graphite" Phys. Rev. 71, 622 (1947).
C. Berger, Z. Song, X. Li, X. Wu, N. Brown, C. Naud, D. Mayou, T. Li, J. Hass, A. N. Marchenkov, E. H. Conrad, P. N. First, W. A. de Heer "Electronic Confinement and Coherence in Patterned Epitaxial Graphene" Science 312 1191 (2006).
J. Fernandéz Rossier, J. J. Palacios "Magnetism in Graphene Nanoislands" Phys. Rev. Lett. 99, 177204 (2007).
Y.-W. Son, M. L. Cohen, S. G. Louie "Half-metallic graphene nanoribbons" Nature 444, 347 (2006).
O. Hod, V. Barone, G. E. Scuseria "Half-metallic graphene nanodots: A comprehensive first-principles theoretical study" Phys. Rev. B 77, 035411 (2008).
D. Yu, E. M. Lupton, H. J. Gao, C. Zhang, F. Liu. "A unified rule for designing nanomagnetism in graphene" Nano Res. 1 497 (2008).
G. Trinquier, N. Suaud, J.-P. Malrieu, "Theoretical study of high-spin polycyclic hydrocarbons" Chem. Europ. J. 16 8762 (2010).
M. Ezawa "Metallic graphene nanodisk: Electronic and magnetic properties" Phys. Rev. B 76, 245415 (2007).
J. A. Fürst, J. G. Pederson, C. Flindt, N. A. Mortensen, M. Brandbyge, T. G. Pedersen, A.-P. Jauho "Electronic Properties of graphene antidot lattice" J. of Phys. 11 095020 (2009).
J. B. Pendry, A. J. Holden, W. J. Stewart I. Youngs "Extremely Low Frequency Plasmons in Metallic Mesostructures" Phys. Rev. Lett. 76 4773 (1996).
O. Hod, J. E. Peralta, G. E. Scuseria Phys. Rev. B "Edge effects in finite elongated graphene nanoribbons" 76, 233401 (2007).
E. H. Lieb "Two theorems on the Hubbard model" Phys. Rev. Lett. 62 1201 (1989)
R. Resta, "Quantum-Mechanical Position Operator in Extended Systems" Phys. Rev. Lett. 80, 1800 (1998).
R. Resta and Sorella, "Electron Localization in the Insulating State" Phys. Rev. Lett. 82, 370 (1999).
S. Evangelisti, G. L. Bendazzoli and A. Monari "Electron localizability and polarizability in tight-binding graphene nanostructures", Theor. Chem. Acc. 126, 257 (2010)
W. Kohn, "Theory of the Insulating State" Phys. Rev. 133, A171 (1964)

Y.Aoki and A. Imamura, "An analytical Hückeltype approach to the relationship between Peierls instability in polyenes and interchain interaction" J. Chem. Phys., 103, 9726 (1995).

R. Resta, "Electron Localization in the Quantum Hall Regime", Phys. Rev. Lett. 95, 196805 (2005).

R. Resta, J. Chem. Phys. "Kohns theory of the insulating state: A quantum-chemistry viewpoint" 124, 104104 (2006).

I. Souza, T. Wilkens, and R. M. Martin, "Polarization and localization in insulators: Generating function approach" Phys. Rev. B 62, 1666 (2000).

V. Vetere, A. Monari, G.L. Bendazzoli, S. Evangelisti, and B. Paulus, "Full configuration interaction study of the metal-insulator transition in model systems: Li_N linear chains (N = 2,4,6,8)" J. Chem. Phys. 128, 024701 (2008).

A. Monari, G. L. Bendazzoli, S. Evangelisti, "The metal-insulator transition in dimerized Hückel chains" J. Chem. Phys. 129, 134104 (2008)

G. l. Bendazzoli, S. Evangelisti, A. Monari, R. Resta, "Kohns localization in the insulating state: One-dimensional lattices, crystalline versus disordered" J. Chem. Phys. 133, 064703 (2010)

http://www.netlib.org/lapack/

Molpro quantum chemistry package, by P. Knowles and H. J. Werner http://www.molpro.net

W.J. Hehre, R.F. Stewart and J.A. Pople, "SelfConsistent MolecularOrbital Methods. I. Use of Gaussian Expansions of SlaterType Atomic Orbitals" J. Chem. Phys. 51 2657 (1969).

B. O. Roos, P. R.Taylor, P. E. M. Sieghbahn "A complete active space SCF method (CASSCF) using a density matrix formulated super-CI approach" Chem. Phys. 48, 157 (1980).

C. Angeli, R. Cimiraglia, S. Evangelisti, T. Leininger, and J.-P. Malrieu, "Introduction of n-electron valence states for multireference perturbation theory" J. Chem. Phys., 114, 10252, (2001).

C. Angeli, R. Cimiraglia, J.-P. Malrieu, "n-electron valence state perturbation theory: A spinless formulation and an efficient implementation of the strongly contracted and of the partially contracted variants" J. Chem. Phys., 117, 9138, (2002)

C. Angeli, M. Pastore, R. Cimiraglia, Theor. Chem. Acc., "New perspectives in multireference perturbation theory: the n -electron valence state approach" 117, 743 (2007).

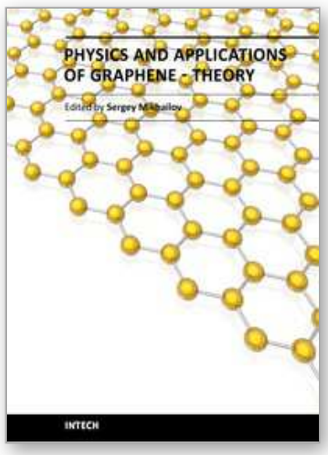

Physics and Applications of Graphene - Theory

Edited by Dr. Sergey Mikhailov

ISBN 978-953-307-152-7
Hard cover, 534 pages
Publisher InTech
Published online 22, March, 2011
Published in print edition March, 2011

The Stone Age, the Bronze Age, the Iron Age... Every global epoch in the history of the mankind is characterized by materials used in it. In 2004 a new era in material science was opened: the era of graphene or, more generally, of two-dimensional materials. Graphene is the strongest and the most stretchable known material, it has the record thermal conductivity and the very high mobility of charge carriers. It demonstrates many interesting fundamental physical effects and promises a lot of applications, among which are conductive ink, terahertz transistors, ultrafast photodetectors and bendable touch screens. In 2010 Andre Geim and Konstantin Novoselov were awarded the Nobel Prize in Physics "for groundbreaking experiments regarding the two-dimensional material graphene". The two volumes Physics and Applications of Graphene - Experiments and Physics and Applications of Graphene - Theory contain a collection of research articles reporting on different aspects of experimental and theoretical studies of this new material.

INTECH
open science | open minds

InTech Europe
University Campus STeP Ri
Slavka Krautzeka 83/A
51000 Rijeka, Croatia
Phone: +385 (51) 770 447
Fax: +385 (51) 686 166
www.intechopen.com

InTech China
Unit 405, Office Block, Hotel Equatorial Shanghai
No.65, Yan An Road (West), Shanghai, 200040, China
中国上海市延安西路65号上海国际贵都大饭店办公楼405单元
Phone: +86-21-62489820
Fax: +86-21-62489821

IntechOpen